

Spectroscopic signatures of massless gap opening in graphene

L. Benfatto^{1,2,3} and E. Cappelluti^{2,3}

¹*Centro Studi e Ricerche "Enrico Fermi," via Panisperna 89/A, I-00184 Rome, Italy*

²*SMC-INFM, CNR-INFM, via dei Taurini 19, 00185 Roma, Italy*

³*Dipartimento di Fisica, Università "La Sapienza," Piazzale Aldo Moro 2, 00185 Roma, Italy*

(Received 27 June 2008; revised manuscript received 25 August 2008; published 26 September 2008)

Gap opening in graphene is usually discussed in terms of a semiconductinglike spectrum, where the appearance of a finite gap at the Dirac point is accompanied by a finite mass for the fermions. In this paper we propose a gap scenario from graphene which preserves the massless characters of the carriers. This approach explains recent spectroscopic measurements carried out in epitaxially grown graphene, ranging from photoemission to optical transmission.

DOI: [10.1103/PhysRevB.78.115434](https://doi.org/10.1103/PhysRevB.78.115434)

PACS number(s): 73.63.-b, 71.10.Pm, 71.30.+h, 81.05.Uw

I. INTRODUCTION

In the last few years the realization of free-standing single layers of graphene opened a new route to the possibility of investigating the behavior of massless Dirac fermion in two dimensions. Indeed, in graphene the valence and conduction bands are formed by the p_z orbitals of the carbon atoms arranged on the two sublattices A and B of the honeycomb lattice. When the two sublattices are electrostatically equivalent the two bands meet at the K (K') points of the Brillouin zone, leading to a zero-gap semiconductor with two conical bands $\varepsilon_k^\pm = \pm v_F k$ ($k = |\mathbf{k}|$), which resemble relativistic Dirac carriers with zero mass and Fermi velocity v_F . For this reason, K and K' are usually referred to as Dirac points. Even though the massless Dirac spectrum makes graphene the perfect playground for investigating relativistic effects in quantum systems, for device application a tunable-gap semiconducting behavior would be more suitable. Along this perspective, of remarkable interest are some recent experiments of angle-resolved photoemission spectroscopy (ARPES) in epitaxially grown graphene, which reveal a finite band splitting $2\Delta \sim 0.26$ eV at the K point.^{1,2} In these works the authors propose that the splitting arises from the inequivalence of the A and B sublattices, which in turn leads to a massive (ms) gapped spectrum:^{3,4}

$$E_{k,\pm}^{\text{ms}} = \pm \sqrt{(v_F k)^2 + \Delta^2}. \quad (1)$$

The magnitude of the band-splitting gap has been reported to decrease by increasing the number of layers, or, from another perspective, by reducing the induced charge density. Similar ARPES spectra were reported previously in Ref. 5, although a different interpretation was proposed.⁵⁻⁷ The most convincing argument in such a controversy comes from the electronic dispersion far from the Dirac point, which is at odds with the massive gapped spectrum of Eq. (1). Indeed, Eq. (1) predicts $E_{k,\pm}^{\text{ms}}$ to be unaffected by the gap opening in the $|E_{k,\pm}^{\text{ms}}| \gg \Delta$ regime, and in particular the linear asymptotic behavior of the upper band $E_{k,+}^{\text{ms}} \approx v_F k$ ($E_{k,+}^{\text{ms}} \gg \Delta$) should match the linear behavior of the lower band $E_{k,-}^{\text{ms}} \approx -v_F k$. A careful analysis of the ARPES data reveals on the contrary a finite off-shift of the two asymptotic linear behaviors,^{1,2,5,6} which cannot be explained even by the periodic modulation induced by the substrate.⁸ Further discrepancies appear also in

the profile of the dispersion at finite k_x away from the K point (Ref. 1, Fig. S3): Instead of the parabolic shape predicted by Eq. (1), a "V" shaped conic profile appears, characteristic of a massless dispersion.

Quite remarkably, the issue of the gap opening has been raised also by very recent optical-absorption measurements in epitaxial graphene.⁹ Indeed, the analysis of the optical spectra based on the massive gap model (1) has two major drawbacks: From one side, it would suggest that no gap (or a negligible one) is present in the system, in contrast with ARPES results; from the other side it fails in reproducing the data in the visible frequency range, where the "universal" conductivity value of $e^2/4\hbar$ is expected theoretically,¹⁰⁻¹² and tested experimentally in multilayer graphite samples¹³ or few-layers suspended graphene.¹⁴ The aim of this paper is to propose a phenomenological gap scenario that reconciles the gapped nature of the spectrum with the massless character of the fermions in graphene. As we shall see, such a gap model not only accounts very well for the ARPES spectra, but explains also optical measurements performed from the visible to the far-infrared (IR) regime.

II. OFF-DIAGONAL SELF-ENERGY CORRECTIONS

Let us start by introducing the Hamiltonian for free electrons in the graphene honeycomb lattice, in terms of the usual spinor $\psi_{\mathbf{k}}^\dagger = (c_{\mathbf{k},A}^\dagger, c_{\mathbf{k},B}^\dagger)$. Linearizing around the K Dirac point (we put $\hbar = 1$), and using $\mathbf{k} = k(\cos \phi, \sin \phi)$, we can write

$$\hat{H}_{\mathbf{k}}^0 = v_F k \begin{pmatrix} 0 & e^{-i\phi} \\ e^{i\phi} & 0 \end{pmatrix}, \quad (2)$$

whose eigenvalues are the usual gapless Dirac cones $\varepsilon_k^\pm = \pm v_F k$. If the A and B sublattices are electrostatically inequivalent, an additional term $\propto \Delta \hat{\sigma}_z$ ($\hat{\sigma}_{i=L,x,y,z}$ being the Pauli matrices) should be added to $\hat{H}_{\mathbf{k}}^0$, and the gapped spectrum of Eq. (1) is recovered. In a similar way, in Ref. 4 it was shown that a gap opening, related to intervalley scattering, is always associated with a mass onset. Finally, off-diagonal intravalley processes of the kind $Q_1^x \hat{\sigma}_x + Q_1^y \hat{\sigma}_y$ were claimed to lead to a mere displacement of the Dirac cone off the K (K') points.⁴ However, this statement is correct only as far as

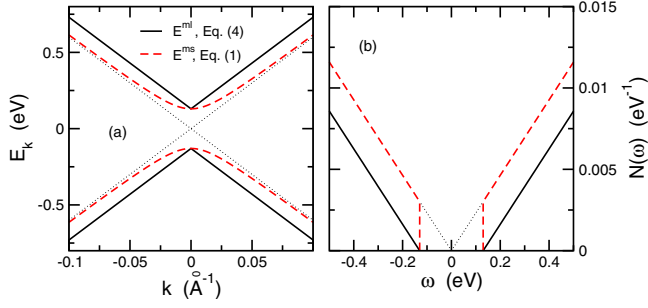


FIG. 1. (Color online) Electronic dispersion (a) and DOS (b) for the massless E^{ml} (solid black line) and massive E^{ms} (dashed red line) gapped models, with $\Delta=0.13$ eV. The dotted line refers to the Dirac-type dispersion ε in the absence of any gap.

a constant value of Q_1^x, Q_1^y for $\mathbf{k} \rightarrow 0$ is assumed, while in general a momentum dependence of the off-diagonal self-energy cannot be ruled out. For instance, the (unscreened) Coulomb interaction leads to the off-diagonal self-energy $\hat{\Sigma}_{\mathbf{k}} \propto k \log(k_c/k) [\cos \phi \hat{\sigma}_x + \sin \phi \hat{\sigma}_y]$, where k_c is a momentum cutoff for the Dirac-type conical behavior.¹⁵ In this case, a correction to the linear Dirac dispersion is achieved, but no gap opens because $\hat{\Sigma}$ vanishes as $k \rightarrow 0$.

In this paper we want to explore a somehow intermediate possibility, where the off-diagonal self-energy has the structure

$$\hat{\Sigma}_{\mathbf{k}} \approx \Delta [\cos \phi \hat{\sigma}_x + \sin \phi \hat{\sigma}_y]. \quad (3)$$

It is straightforward to check that, in this case, a gap is opened at the K (K') points without the onset of a massive term. Indeed, Eq. (3) leads to the massless (ml) gapped spectrum of the form

$$E_{k,\pm}^{\text{ml}} = \pm (v_F k + \Delta), \quad (4)$$

with a corresponding density of states (DOS):

$$N(\omega) = \frac{V_{\text{BZ}}}{2\pi v_F^2} (|\omega| - \Delta) \theta(|\omega| - \Delta), \quad (5)$$

where $V_{\text{BZ}} = 5.24 \text{ \AA}^2$ is the volume of the Brillouin zone.

In Fig. 1 we compare the electronic dispersion (panel a) and the DOS (panel b) of models (4) and (1). Two main striking features need here to be stressed: (i) the gap in Eq. (4), as mentioned, is created without affecting the conical electronic dispersion. In this sense no massive term is induced; (ii) in contrast to the case of the massive gap model (1), the lower and upper cones of spectrum (1) are misaligned by the quantity 2Δ . Such anomalous features are reflected in the DOS [Eq. (5)] where the linear vanishing of $N(\omega)$ as $|\omega| \rightarrow \Delta^+$ in model (4) points out the absence of a quadratic massive term, while the misalignment of the cones is reflected in a corresponding mismatch of the linear dependence of the DOS, which does not extrapolate to zero at the Dirac point.

Even though the aim of this paper is to focus on the outcomes of the phenomenological spectrum (4), it is worth discussing the basic features of the microscopic model that can lead to the proposed effects. Within a Hartree-Fock approach, we can write the self-energy as

$$\hat{\Sigma}(\mathbf{k}) = -V \sum_{\mathbf{k}', i\omega_n} F(\mathbf{k} - \mathbf{k}') \hat{G}(\mathbf{k}', i\omega_n) e^{i\omega_n 0^+}, \quad (6)$$

where \hat{G} is the electronic Green's function, V is the strength of the electronic interaction, and $F(\mathbf{q})$ is a form factor which depends in general on both the modulus and direction of the exchanged momentum \mathbf{q} . In the experiments the gap is clearly observed only in doped samples when the chemical potential μ is far enough from the Dirac point and the screening due to the finite density of states makes the interaction short-ranged. In first approximation, this is usually described in terms of a completely isotropic form factor F . Here however we shall consider the case where this residual scattering is not completely isotropic, but it retains a dependence on the azimuthal angles ϕ and ϕ' which favors forward scattering. Such angle anisotropy can be parametrized for example as $F(\phi - \phi') = \Theta(\phi_c - |\phi - \phi'|)$, where $\Theta(x)$ is the Heaviside function and where $\phi_c = \pi$ corresponding to isotropic scattering. To compute self-energy (6) it is useful to make explicit the angle dependence of the Green's function \hat{G} , which can be easily deduced from Eq. (2):

$$\hat{G}(k, \phi, i\omega_n) = G_+(k, i\omega_n) \hat{I} + G_-(k, i\omega_n) [\cos(\phi) \hat{\sigma}_x + \sin(\phi) \hat{\sigma}_y], \quad (7)$$

where G_{\pm} are functions of k only. For example, for the bare Green's function \hat{G}_0 is $G_{\pm} = [(i\omega_n + \mu - v_F k)^{-1} \pm (i\omega_n + \mu + v_F k)^{-1}] / 2$. By means of Eq. (6) one sees that the self-energy correction (and then the dressed Green's function \hat{G}) preserves the same structure (7) as far as the angle dependence and matrix structure is concerned. By decomposing $\hat{\sigma}$ in the Pauli matrices:

$$\hat{\Sigma}(\phi) = \Sigma_I \hat{I} + \Sigma_x(\phi) \hat{\sigma}_x + \Sigma_y(\phi) \hat{\sigma}_y, \quad (8)$$

one finds that Σ_I can be absorbed in a redefinition of the chemical potential, while the terms proportional to $\hat{\sigma}_{x,y}$ scale as $\cos(\phi)$ and $\sin(\phi)$, respectively. For example,

$$\begin{aligned} \Sigma_x(\phi) &= -V \int \frac{d^2 \mathbf{k}'}{(2\pi)^2} F(\phi - \phi') \cos(\phi') [n_+(k') - n_-(k')] \\ &\approx \cos \phi \frac{V \sin \phi_c}{2} \left(\frac{k_c}{2\pi} \right)^2 = \Delta \cos \phi, \end{aligned} \quad (9)$$

where we used the fact that

$$\begin{aligned} &\int \frac{d\phi'}{2\pi} \Theta(\phi_c - |\phi - \phi'|) \cos \phi' \\ &= \frac{1}{2\pi} [\sin(\phi + \phi_c) - \sin(\phi - \phi_c)] \\ &= \frac{\sin \phi_c}{\pi} \cos \phi. \end{aligned}$$

Observe that the Matsubara sum in Eq. (9) gives rise to the difference of the occupation numbers $n_{\pm}(k)=f(E_{k,\pm}^{\text{ml}}-\mu)$ of the upper and lower bands, respectively, where $f(x)$ is the Fermi function. Thus, evaluating them with the bare or dressed Green's function gives only a difference in the prefactor, which is $(v_F k_c)^2 - \mu^2$ in the former case and $(v_F k_c)^2 - (\mu - \Delta)^2$ in the latter case, μ being the chemical potential. However, since usually $v_F k_c \gg \mu, \Delta$ we simply approximated it with $v_F k_c$. It is worth noting that if $\Delta < 0$ one does not have a gap, but one simply obtains a shift of the Dirac point.⁴ This is the case for (anisotropic) scattering of electrons by impurities. Indeed, self-energy corrections due to scattering by impurities evaluated in the usual Born approximation correspond to an attractive effective interaction between electrons,^{16,17} so that they would lead to a negative Δ value. The same result holds for scattering by phonons, unless they are coupled as $\hat{\sigma}_z$ in spinor space. As far as the scattering of electrons by the collective mode associated with mesoscopic corrugations of the graphene plane is concerned, the existing calculations suggest strong (local) velocity renormalization,¹⁸ but not directly a gap opening. However, as the previous example suggests an intrinsic anisotropy of the scattering process is required to produce off-diagonal self-energy correction, so that further investigation is required to establish if ripples can be the source of the proposed model (4).

In addition to the off-diagonal self-energy corrections, all the above-mentioned scattering mechanisms will contribute to Σ_I , giving rise to a finite electron lifetime, that we will parametrize in the following as $\Sigma_I(i\omega_n) = -i\Gamma(i\omega_n)$. Finally, the dressed inverse Green's function \hat{G}^{-1} is

$$\hat{G}^{-1}(\mathbf{k}, i\omega_n) = \begin{pmatrix} z + i\Gamma(i\omega_n) & (v_F k + \Delta)e^{-i\phi} \\ (v_F k + \Delta)e^{i\phi} & z + i\Gamma(i\omega_n) \end{pmatrix}, \quad (10)$$

where $z = i\omega_n + \mu$, so that the spectral function reads

$$A(\mathbf{k}, \omega) = \frac{\Gamma}{(2\pi)} \left\{ \frac{1}{(\omega - \mu - v_F k - \Delta)^2 + \Gamma^2} + \frac{1}{(\omega - \mu + v_F k + \Delta)^2 + \Gamma^2} \right\}.$$

III. COMPARISON WITH THE EXPERIMENTS

To make a comparison with the ARPES results in epitaxially grown graphene, we show in Fig. 2(a) the calculated spectral intensity $I(\mathbf{k}, \omega) = A(\mathbf{k}, \omega)f(\omega)$ as a function of k_x at $k_y=0$ where $f(\omega)$ is the Fermi function, and we used $\mu=0.4$ eV and $2\Delta=0.26$ eV.¹ For the sake of comparison with the experiments we assumed a quasiparticle scattering rate $\Gamma(\omega) = \Gamma_0 + \alpha|\omega|$, with $\Gamma_0=0.165$ eV and $\alpha=0.11$ fitted from the ARPES data^{2,5} away from the Dirac point using $v_F=6$ eV Å.¹⁹ Notice that the presence of such a large scattering rate at the Dirac point partly spoils the gap feature as $k \rightarrow 0$, because the two peaks of $A(\mathbf{k}=0, \omega)$ at $\omega = \pm \Delta$ significantly overlap, as shown also by the energy-distribution curves (cuts of the intensity map at a constant momentum) reported in Fig. 2(b). In the experiments, where the scatter-

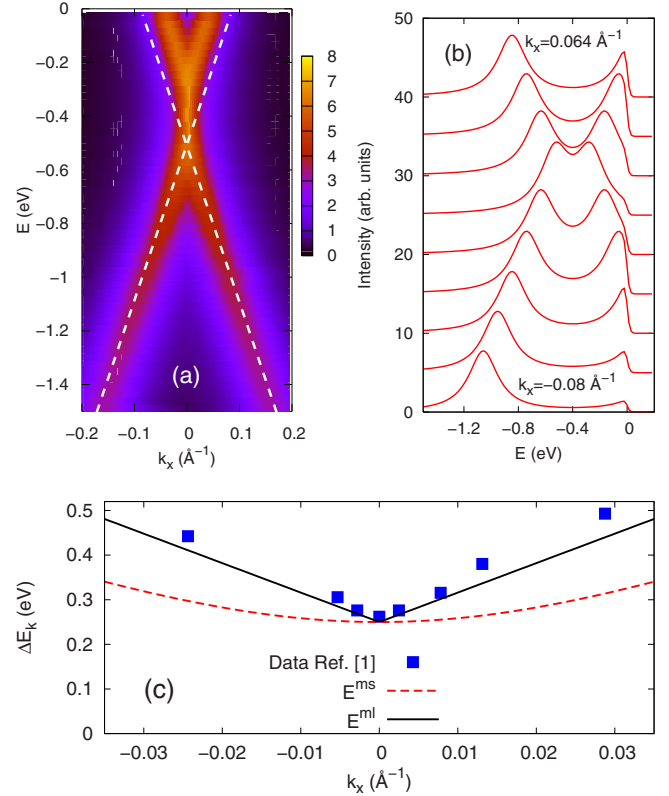


FIG. 2. (Color online) (a) Intensity map of the spectral function $A(k_x, k_y=0, \omega)$ of the massless model [Eq. (4)] for $\Delta=0.13$ eV, $v_F=6$ eV Å, and Γ taken from the experiments (see text). Dashed white lines show the mismatch between the asymptotic linear behavior of the upper and lower bands. (b) Corresponding energy-distribution curves taken for $k_y=0$ and equally spaced k_x values. The curves are vertically displaced for clarity. (c) Plot of the gap edge at finite k_x for the massless and massive gap model [Δ, v_F as in panel (a)]. Dark squares are experimental data taken from Ref. 1.

ing rate at the Dirac point is even larger than what used here, the two peaks overlap completely and they cannot be resolved, leading to the controversial interpretation of similar ARPES spectra in Refs. 5 and 6 and Refs. 1 and 2, respectively. Nevertheless, one can still clearly resolve in the intensity map of Fig. 2(a) the net misalignment between the upper and lower Dirac cones, which is peculiar to model (4), and is in perfect agreement with all the existing experimental data.^{1,2,5} Moreover, ARPES data taken away from the K point provide us also with a direct evidence of the linear (massless) behavior of the electronic dispersion at finite k . By measuring the dispersion at $k_y=0$ and finite k_x , as extracted from several k_y cuts through the K point, one can easily discriminate between the two models (1) and (4). Indeed, within model (1) the energy spectrum $\sqrt{\Delta^2 + (v_F k_x)^2}$ would appear parabolic within a momentum window $k_x \lesssim \Delta/v_F \approx 0.02$ Å⁻¹, while within the massless model (4) one expects a linear increase in the gap, $\Delta + v_F |k_x|$. The experimental data of Ref. 1 (Fig. S3 in Supplementary material) are reported in Fig. 2(c): As one can see, the massive model E_{\pm}^{ms} shows no resemblance with the data, while the massless model E_{\pm}^{ml} allows one an excellent fit of the dispersion without any adjustable parameter.

The massless character of the spectrum has also significant consequences on the structure of the optical conductivity $\sigma(\Omega)$. To elucidate this issue we evaluate here the optical conductivity in the bare-bubble approximation. As usual, $\sigma(\Omega)$ is given by two parts, associated with intraband and interband transitions.^{10,11} At the leading order in $\Gamma/|\mu|, \Gamma/\Delta \ll 1$, we obtain

$$\begin{aligned} \sigma_{\text{intra}}(\Omega) &= -\frac{e^2}{\pi\hbar} \frac{2\Gamma}{\Omega^2 + 4\Gamma^2} \\ &\times \int d\omega \frac{df(\omega - \mu)}{d\omega} (|\omega| - \Delta) \theta[|\omega| - \Delta] \\ &\approx \frac{e^2}{T \rightarrow 0} \frac{\delta(\Omega) (|\mu| - \Delta) \theta[|\mu| - \Delta]}{\hbar}, \end{aligned} \quad (11)$$

$$\begin{aligned} \sigma_{\text{inter}}(\Omega) &= \frac{e^2}{\pi\hbar} \int d\omega \frac{f(\omega - \mu) - f(\omega + \Omega - \mu)}{4\Omega} \\ &\times \frac{2\Gamma}{(\omega + \Omega/2)^2 + 4\Gamma^2} (|\Omega| - 2\Delta) \theta[|\Omega| - 2\Delta] \\ &\approx \frac{e^2}{T \rightarrow 0} \frac{1}{4\hbar} \left(1 - \frac{2\Delta}{|\Omega|}\right) \theta[|\Omega| - 2 \max(\Delta, |\mu|)]. \end{aligned} \quad (12)$$

As one can see, the general structure of the optical conductivity is the same for all the gapped and ungapped models: a Drude peak of width $\Gamma_{\text{opt}} = 2\Gamma$ and an interband contribution which starts at a threshold given by the larger between 2μ and 2Δ , and saturates at $\Omega \gg \Delta, |\mu|$ to the universal value $e^2/4\hbar$.¹⁰⁻¹² When a gap opens, part of the spectral weight is transferred to the interband transitions and the Drude peak decreases with respect to the ungapped case. In model (1), $\sigma(\Omega)$ can be obtained by replacing the factors $(|\mu| - \Delta) \rightarrow (|\mu| - \Delta^2/|\mu|)$ and $(1 - 2\Delta/|\Omega|) \rightarrow (1 + 4\Delta^2/|\Omega|^2)$, respectively, in Eqs. (11) and (12).^{10,11} Two features allow thus one to differentiate models (1) and (4): the relative weight of interband and intraband contributions and the shape of the conductivity at the interband threshold. In particular, one can see that (i) the gap-induced reduction in the Drude peak is much stronger in the massless gap model (of order $\sim \Delta$) than in the massive one (of order $\sim \Delta^2/|\mu|$) [see inset of Fig. 3(a)]; (ii) while the massive gap model would give rise to a *peak* above the asymptotic value $e^2/4\hbar$ at the edge of the interband spectrum and to a rapid saturation to the asymptotic value, the massless model predicts a *depletion* in the correspondence of such edge (due to the factor $1 - 2\Delta/\Omega < 1$), followed by a slow saturation to the universal value [see Fig. 3(a)]. Such a depletion is again a consequence of the vanishing of the DOS at the gap in the massless model [see Fig. 1(b)], with consequent reduction in the spectral weight for transitions occurring between the two bands.

Thus, the present results open a different perspective in the analysis of the optical properties of graphene grown epitaxially on SiC substrates, which can be deduced from measurements of the optical transmission $T(\omega)$, which in first approximation is related to the real part of the single-layer optical conductivity as $T(\omega) = [1 + N\sigma(\omega)\sqrt{\mu_0/\epsilon_0}/(1 + n_{\text{SiC}})]^{-2}$,^{9,12} where n_{SiC} is the refractive index of SiC and N

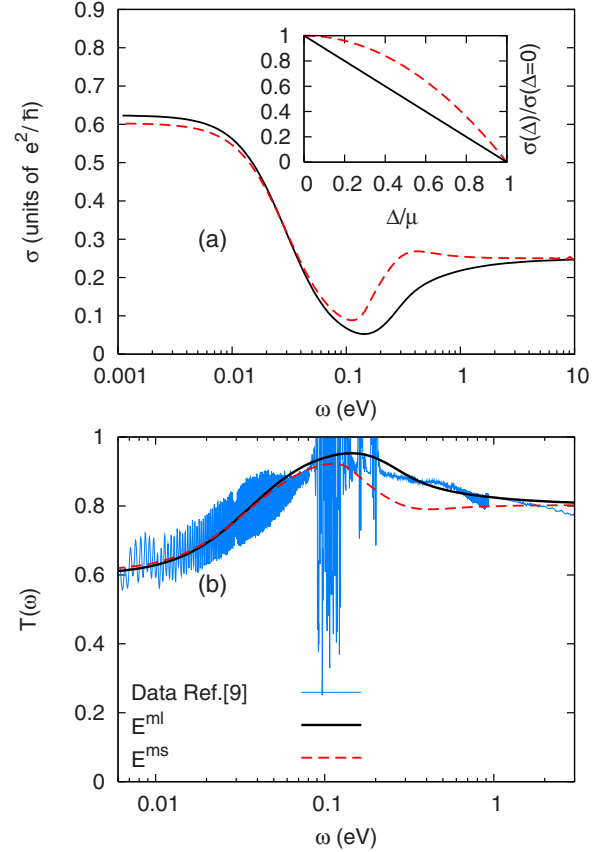


FIG. 3. (Color online) (a) Optical conductivity $\sigma(\Omega)$ for $\mu = 0.1$ eV, $T = 300$ K, and $\Gamma = 15$ meV for the massless gap model (solid black line, $\Delta = 45$ meV) and for the massive gap model (dashed red line, $\Delta = 73$ meV). Inset: reduction in the zero-frequency optical conductivity in the two cases, as a function of Δ/μ . (b): Comparison of the two models with the experimental data for $T(\omega)$ from Ref. 9.

is the number of layers. In Ref. 9, indeed, transmission data for few-layer graphene samples in the frequency range from the far-IR to the visible were analyzed within the context of the massive gap model described in Eq. (1), and the gap was concluded to be negligible within the experimental accuracy $\Delta \leq \Gamma_{\text{opt}} \approx 10$ meV.⁹ Such a fit reproduces the data in the far-IR to mid-IR range, but fails in the visible range, where, according to this fit, the data would then indicate a conductivity *larger* than the universal value $e^2/4\hbar$. The failure of the fit follows from the fact that the size of optical transmission $T(\Omega)$ at $\Omega \approx 3$ eV and for $\Omega \rightarrow 0$, and hence the size of the optical conductivity in the corresponding range, are found to be of the same magnitude. According to the previous discussion, this could be achieved by a transfer of spectral weight from the Drude peak to the interband conductivity, as due to a gap opening. However, to reproduce this feature within the massive gap model one would need $\Delta \approx |\mu| \sqrt{1 - \pi\Gamma/2|\mu|} = 87$ meV, where $|\mu| \approx 0.1$ eV, $\Gamma = \Gamma_{\text{opt}}/2 \approx 15$ meV are extracted from the interband edge and from the width of the Drude peak.⁹ With such large value, $\Delta \gg \Gamma$, the massive gap would be clearly detectable as a sharp peak at the interband edge, which is instead absent in the data. For this reason, the authors of Ref. 9 extracted a

vanishing gap from the fit based on model (1), which then fails in reproducing the data in the visible range.

Such ambiguity can be naturally solved within the context of the massless gap model, where (i) a relatively smaller gap value is needed to make the low- and high-frequency optical conductivity of the same magnitude; (ii) the opening of a massless gap does not give rise to any peak at the threshold of interband transitions but to a *depletion* of the conductivity with respect to the universal value, and then to a slow and smooth crossover toward the high-frequency regime, as observed in the data. This picture is in very good agreement with the actual experimental measurements. In Fig. 3(b) we show the best fit to one set of the experimental data of Ref. 9 by using the massless gap model. We take $|\mu|=0.1$ eV, $T=300$ K, and $\Gamma=15$ meV from the experiments themselves and we estimate $\Delta=45$ meV, $N=18$. For comparison, the fit with the massive gap model, constrained to reproduce the experimental values of $T(\omega)$ in the low- and high-frequency limit, would give $\Delta=73$ meV and $N=18$, and would result in a clear peak (shoulder) at the interband edge. We would like to stress that even though the absence of an interband peak can also be accounted for by a vanishing gap, the similar magnitude of the low- and high-frequency values of the optical transmission is a clear indication of a reduced

Drude height, and hence of the presence of a gap.

IV. CONCLUSIONS

In summary, we propose a gapped model for graphene which allows one to reconcile the massless Dirac character of the carriers with the effects related to a gap opening at the Dirac point. We show that both ARPES and optical-conductivity measurements give clear indications of such massless gap opening in epitaxially grown graphene. Since ARPES measurements are available only for epitaxially grown graphene, we cannot rule out the possibility that such a gap opening is restricted to these systems. Recent tunneling data on epitaxially grown²⁰ and suspended graphene²¹ are not conclusive on this respect; however, our predictions can be further tested experimentally and, if confirmed, they would pose stringent constraints on the interaction mechanisms at play in graphene.

ACKNOWLEDGMENTS

We acknowledge useful discussions with L. Boeri, A. Kuzmenko, and S. G. Sharapov. We thank the authors of Ref. 9 for providing us with the experimental data.

-
- ¹S. Y. Zhou, G.-H. Gweon, A. V. Fedorov, P. N. First, W. A. de Heer, D.-H. Lee, F. Guinea, A. H. Castro Neto, and A. Lanzara, *Nat. Mater.* **6**, 770 (2007).
- ²S. Y. Zhou, D. A. Siegel, A. V. Fedorov, and A. Lanzara, *Physica E (Amsterdam)* **4**, 2642 (2008).
- ³V. P. Gusynin, S. G. Sharapov, and J. P. Carbotte, *Int. J. Mod. Phys. B* **21**, 4611 (2007).
- ⁴J. L. Mañes, F. Guinea, and M. A. H. Vozmediano, *Phys. Rev. B* **75**, 155424 (2007).
- ⁵A. Bostwick, T. Ohta, T. Seyller, K. Horn, and E. Rotenberg, *Nat. Phys.* **3**, 36 (2007).
- ⁶A. Bostwick, T. Ohta, J. L. McChesney, K. V. Emtsev, T. Seyller, K. Horn, and E. Rotenberg, *New J. Phys.* **9**, 385 (2007).
- ⁷E. Rotenberg, A. Bostwick, T. Ohta, J. L. McChesney, Th. Seyller, and K. Horn, *Nat. Mater.* **7**, 258 (2008); S. Y. Zhou, D. A. Siegel, A. V. Fedorov, F. El Gabaly, A. K. Schmid, A. H. Castro Neto, D.-H. Lee, and A. Lanzara, *ibid.* **7**, 259 (2008).
- ⁸S. Kim, J. Ihm, H. J. Choi, and Y.-W. Son, *Phys. Rev. Lett.* **100**, 176802 (2008).
- ⁹J. M. Dawlaty, S. Shivaraman, J. Strait, P. George, Mvs. Chandrashekar, F. Rana, M. G. Spencer, D. Veksel, and Y. Chen, arXiv:0801.3302 (unpublished).
- ¹⁰T. Ando, Y. Zheng, and H. Suzuura, *J. Phys. Soc. Jpn.* **71**, 1318 (2002).
- ¹¹V. P. Gusynin, S. G. Sharapov, and J. P. Carbotte, *Phys. Rev. Lett.* **96**, 256802 (2006).
- ¹²T. Stauber, N. M. R. Peres, and A. K. Geim, *Phys. Rev. B* **78**, 085432 (2008).
- ¹³A. B. Kuzmenko, E. van Heumen, F. Carbone, and D. van der Marel, *Phys. Rev. Lett.* **100**, 117401 (2008).
- ¹⁴R. R. Nair, P. Blake, A. N. Grigorenko, K. S. Novoselov, T. J. Booth, T. Stauber, N. M. R. Peres, and A. K. Geim, *Science* **320**, 1308 (2008).
- ¹⁵E. G. Mishchenko, *Phys. Rev. Lett.* **98**, 216801 (2007).
- ¹⁶G. D. Mahan, *Many-Particle Physics* (Plenum, New York, 1981).
- ¹⁷N. H. Shon and T. Ando, *J. Phys. Soc. Jpn.* **67**, 2421 (1998).
- ¹⁸F. de Juan, A. Cortijo, and M. A. H. Vozmediano, *Phys. Rev. B* **76**, 165409 (2007); A. Cortijo and M. A. H. Vozmediano, arXiv:0709.2698 (unpublished).
- ¹⁹A. H. Castro Neto, F. Guinea, N. M. R. Peres, K. S. Novoselov, and A. K. Geim, arXiv:0709.1163, *Rev. Mod. Phys.* (to be published).
- ²⁰L. Vitali, C. Riedl, R. Ohmann, I. Brihuega, U. Starke, and K. Kern (unpublished).
- ²¹G. Li, A. Luican, and E. Y. Andrei, arXiv:0803.4016 (unpublished).